

Type IIb supernovae by the grazing envelope evolution

Binyamin V. Naiman¹ Efrat Sabach^{1*}, Avishai Gilkis^{2†}, Noam Soker^{1,3‡}

¹ *Department of Physics, Technion – Israel Institute of Technology, Haifa 3200003, Israel*

² *Institute of Astronomy, University of Cambridge, Madingley Road, Cambridge, CB3 0HA, UK*

³ *Guangdong Technion Israel Institute of Technology, Shantou, Guangdong Province 515069, China*

4 September 2022

ABSTRACT

We simulate the evolution of binary systems with a massive primary star of $15M_{\odot}$ where we introduce an enhanced mass loss due to jets that the secondary star might launch, and find that in many cases the enhanced mass loss brings the binary system to experience the grazing envelope evolution (GEE) and form a progenitor of Type IIb supernova (SN IIb). The jets, the Roche lobe overflow (RLOF), and a final stellar wind remove most of the hydrogen-rich envelope, leaving a blue-compact SN IIb progenitor. In many cases without this jet-driven mass loss the system enters a common envelope evolution (CEE) and does not form a SN IIb progenitor. We use the stellar evolutionary code MESA BINARY and mimic the jet-driven mass loss with a simple prescription and some free parameters. Our results show that the jet-driven mass loss, that some systems have during the GEE, increases the parameter space for stellar binary systems to form SN IIb progenitors. We estimate that the binary evolution channel with GEE contributes about a quarter of all SNe IIb, about equal to the contribution of each of the other three channels, binary evolution without a GEE, fatal CEE (where the secondary star merges with the core of the giant primary star), and the single star channel.

Key words: stars: jets — stars: supernovae: general — binaries: close — accretion disks

1 INTRODUCTION

1.1 Type IIb supernovae (SNe IIb)

Supernovae IIb (SNe IIb) are classified as core collapse supernovae (CCSNe) that have strong hydrogen lines at early times, days after explosion, which later substantially weaken and even disappear. The weakening of the hydrogen lines results from a low mass hydrogen-rich envelope of the SN IIb progenitor. This behaviour implies that the progenitor of the CCSN has a very small hydrogen mass at the time of explosion, $M_{\text{H}} \simeq 0.03 - 0.5M_{\odot}$ (e.g., Woosley et al. 1994; Meynet et al. 2015; Yoon et al. 2017). In their population synthesis study Sravan et al. (2018) take the hydrogen-rich envelope of the progenitor at the onset of explosion to have a mass of $0.01M_{\odot} \leq M_{\text{H,env}} \leq 1M_{\odot}$.

SNe IIb amount to about $f_{\text{IIb}} \simeq 11\%$ of all CCSNe (Smith et al. 2011; Shivvers et al. 2017; Graur et al. 2017b). Graur et al. (2017b) find that the relative rates of SNe IIb do not depend much on the mass of their host galaxies. Sravan

et al. (2018) take $f_{\text{IIb,H}} \simeq 10-12\%$ in high metallicity stellar populations and $f_{\text{IIb,L}} \simeq 20\%$ in low metallicity populations.

There is observational support for the binary scenario for the formation of SNe IIb. Kilpatrick et al. (2017) fit a binary model for the progenitor of SN 2016gkg with an initial period of $P_i = 1000$ days, and initial stellar masses of $M_{1,i} = 15M_{\odot}$ and $M_{2,i} = 1.5M_{\odot}$. The pre-explosion primary mass in their fitting is $M_{1,f} = 5.2M_{\odot}$. Aldering et al. (1994) deduce from the photometry of the SN IIb 1993J that it better fits a binary progenitor, as suggested by Podsiadlowski et al. (1993). Fox et al. (2014) argue that the flattened circumstellar matter around SN 1993J (Matheson et al. 2000) supports a binary progenitor. Fremling et al. (2019) study the SN IIb ZTF18aalrxas, and find its hydrogen mass to be $\approx 0.15M_{\odot}$, and argue that the zero age main sequence (ZAMS) mass of its progenitor was about $12M_{\odot}$. They further find massive CSM, and argue that only a binary interaction can explain all these properties. Soker (2017) takes a mass loss in a flat disk or ring to support the grazing envelope evolution (GEE) route (section 1.2 below), as such a structure is found in Post-asymptotic giant branch intermediate binaries (post-AGBIBs; e.g., Kastner et al. 2010; Van Winckel 2017a), and the main sequence companion in some post-AGBIBs are observed to launch jets (e.g., Witt et al.

* Contact e-mail: efrats@physics.technion.ac.il

† Contact e-mail: agilkis@ast.cam.ac.uk

‡ Contact e-mail: soker@physics.technion.ac.il

2009; Gorlova et al. 2012; Thomas et al. 2013; Gorlova et al. 2015; Van Winckel 2017b). The companion orbits outside but close to the post AGB star.

Claeys et al. (2011) who expand the work of Stancliffe & Eldridge (2009) find that binary evolution predicts only $\approx 0.6\%$ of all CCSNe to be SN I Ib, much lower than the observed fraction. They could increase this fraction if they consider low angular momentum loss from the binary system and low accretion efficiencies by the companion, such that the specific angular momentum lost in the outflow is smaller than that of the binary system. Ouchi & Maeda (2017) also share the conclusion of a large mass loss fraction. Soker (2017) attributes the efficient mass removal from the binary system to jets that the companion star launches as it accretes mass from the SN progenitor. Soker (2017) argues that the jets in the GEE scenario both remove mass from the primary stellar progenitor with relatively low specific angular momentum, and limit mass accretion onto the companion itself.

In their very recent population synthesis study Sravan et al. (2018) find that single and binary progenitors contribute about equally to the population of SNe I Ib. However, they fall short of explaining the rate of SNe I Ib by a factor of more than 3 (also Sravan 2016). Winds that are weaker than usually assumed remove less hydrogen-rich envelope gas after the end of the mass transfer process, and by that can reduce the discrepancy with observations (Gilkis et al. 2019).

The main evolutionary channel that Sravan et al. (2018) consider is Roche lobe overflow (RLOF) mass transfer. We assume that the vast majority, and possibly all, of SNe I Ib are a result of binary interaction. To boost the number of binary progenitors of SNe I Ib we include two more evolutionary channels. The first one is the GEE route, as proposed by Soker (2017) and which is the subject of the present study. The second evolutionary route is that where a main sequence companion ejects all the original hydrogen-rich envelope, and then is destroyed on to the core of the massive star. The secondary star becomes the new low-mass hydrogen-rich envelope of the massive star (Lohev et al. 2019). Lohev et al. (2019) suggest this fatal common envelope evolution (FCEE) scenario to explain the SN I Ib Cassiopeia A.

A useful classification of SNe I Ib progenitors is to extended progenitors (i.e., red supergiants Chevalier, & Soderberg 2010) and compact progenitors. Yoon et al. (2017) discuss blue progenitors, yellow supergiant progenitors, and red supergiant progenitors, and their formation via RLOF. The first two groups are compact and have little hydrogen mass at explosion, $M_H \lesssim 0.15M_\odot$. The hydrogen mass at explosion of the red supergiant progenitors is $M_H \gtrsim 0.15M_\odot$. Both stable and unstable mass transfer can form compact progenitors of SNe I Ib, that make most of the SNe I Ib. The GEE cases that we simulate in the present study lead to the formation of blue-compact SN I Ib progenitors, as post-GEE winds remove most of the hydrogen that is left after the GEE. Yoon et al. (2017) already noted that post-RLOF winds are efficient in removing most of the left-over hydrogen (see also Gilkis et al. 2019). Winds in higher metallicity populations are more efficient in removing mass, therefore leading to a higher ratio of SNe I Ib to SNe I Ib.

Before we turn to mimic the GEE in simulations, we briefly describe the basic properties of the GEE and the

general motivation to introduce the GEE into binary stellar evolution. Soker (2017) presents in more details some of the properties of the GEE that are relevant to the formation of SNe I Ib.

1.2 The grazing envelope evolution (GEE)

There are several results that motivate the introduction of the GEE. (1) The observations of post-AGBIBs, where a secondary star is close but outside the envelope of a post-AGB star (e.g., Manick et al. 2017; Oomen et al. 2018) where traditional evolutionary calculations predict no binary systems (e.g., Nie et al. 2012). (2) The observations that the companion in many post-AGBIBs launches jets, even wide jets (e.g., Thomas et al. 2013). (3) The failure of most hydrodynamical simulations of the common envelope evolution (CEE) to eject the entire envelope in a consistent and persistent manner (e.g., Taam & Ricker 2010; De Marco et al. 2011; Passy et al. 2012; Ricker & Taam 2012; Nandez et al. 2014; Ohlmann et al. 2016; Staff et al. 2016b; Nandez & Ivanova 2016; Kuruwita et al. 2016; Ivanova & Nandez 2016; Iaconi et al. 2017; De Marco & Izzard 2017; Galaviz et al. 2017; Chamandy et al. 2019; Reichardt et al. 2019). These simulations might hint on the need for an extra energy source to eject the envelope.

The GEE posits that this extra energy source is the gravitational energy that is released by mass that the more compact companion accretes, and that jets carry this energy to the ambient gas (Soker 2016 for a review). Blackman & Lucchini (2014) suggest that the high momenta in bipolar planetary nebulae indicate that the companion can launch jets in a CEE. From the theoretical side, the energy and the high entropy gas that the jets themselves can carry away from the accretion flow allows a high accretion rate (e.g., Shiber et al. 2016; Staff et al. 2016a; Chamandy et al. 2018). Without this energy removal the gas would build a high pressure zone near the accreting object. Such a high pressure zone reduces the accretion rate (e.g. Ricker & Taam 2012; MacLeod & Ramirez-Ruiz 2015).

In the GEE jets that the more compact secondary star launches as it grazes the envelope of a giant star remove mass from the envelope (Sabach & Soker 2015; Soker 2015; Shiber et al. 2017; Shiber & Soker 2018; López-Cámara et al. 2019; Shiber et al. 2019). The GEE occurs when the jets efficiently remove mass from the giant envelope near the orbit of the companion. Such a mass removal can delay, and even prevent, the full CEE. The interplay between mass loss, mass accretion, and mass removal by jets determines which one of these outcomes takes place. (1) The system enters a CEE. (2) The orbital separation substantially decreases as the binary system experiences the GEE. (3) The orbital separation does not change by much. (4) The orbital separation somewhat increases.

We would like to emphasise the differences between the GEE, that we propose as one of the main channels to form SN I Ib progenitors, and the case of a RLOF that is usually discussed in the literature (section 1.1). (1) In the RLOF process the gravity of the companion and the winds remove mass from the giant envelope. Therefore, if the system loses synchronisation or if the giant expands further, the RLOF process by itself would not be able to prevent the system from entering a CEE. In the GEE the extra energy source

that the jets supply can remove more envelope mass and in some cases prevent the CEE. The GEE, hence, substantially increases the parameter space for the formation of SNe I Ib. (2) In the RLOF process most of the mass flows through the first Lagrangian point. In the GEE the accretion process on to the companion is a combination of a RLOF and a Bondi-Hoyle-Lyttleton type accretion. (3) In the RLOF process the companion orbits well outside the giant envelope, while in the GEE the companion grazes the giant envelope. We note that on average the orbital separation during the GEE can be smaller than the radius of the giant star since in the vicinity of the secondary star the jets remove envelope mass and the edge of the envelope at the secondary location is smaller.

Our goal is to show that the GEE can increase the parameter space for the formation of SNe I Ib. Namely, to show that the jets of the GEE can prevent systems that otherwise would have entered a CEE from entering a CEE, and that the hydrogen mass at core collapse in some of these systems is that expected for SNe I Ib. In this, still preliminary, study we mimic the GEE by changing the parameters of mass transfer and mass loss with the MESA BINARY code. In section 2 we describe our numerical scheme to mimic the GEE, and in section 3 we present our results. We summarise in section 4.

2 MIMICKING THE GRAZING ENVELOPE EVOLUTION

We use the BINARY module of the MESA code (Modules for Experiments in Stellar Astrophysics, version 10398; Paxton et al. 2011, 2013, 2015, 2018) to follow the evolution of binary systems. Since our goal is to demonstrate that the GEE can extend the binary parameter space for the formation of SNe I Ib, we limit the study to a small number of cases and to circular orbits. We are not yet in a stage that allows us to explore the absolute number of SNe I Ib that result from the GEE channel, because we did not converge yet on the exact scheme to use for jet-driven mass loss. This is the second study of the GEE with MESA BINARY, and we differ quite a lot from the scheme used in the first study with MESA BINARY (Abu-Backer et al. 2018).

We evolve a binary system starting with two main sequence stars of ZAMS masses of $M_{1,0} = 15M_{\odot}$ (the primary mass donor star) and a secondary star with an initial mass of $M_{2,0} = 2.5M_{\odot}$ in most cases, while in some cases $M_{2,0} = 2.0M_{\odot}$ and $M_{2,0} = 3.0M_{\odot}$. The initial metallicity of the primary star is $Z = 0.019$ and its initial rotation velocity is zero. We treat the secondary star as a point mass and do not follow its evolution or change of structure as a result of mass accretion (see Abu-Backer et al. 2018). We set the initial orbital separation to be in the range of $a = 800 - 1200R_{\odot}$.

The system evolves according to mass loss, mass transfer, and tidal interaction (from Hut 1981, with the timescales of Hurley et al. 2002 for convective envelopes). These interactions can spin-up the primary star. In that case the numerical code treats rotation according to the ‘shellular approximation’, where the angular velocity ω is assumed to be constant for isobars (e.g., Meynet & Maeder 1997).

If the stars achieve contact, i.e., the separation equals

the sum of their radii,

$$a = R_1 + R_2, \quad (1)$$

where in our simulations here $R_2 = 0$, in most cases we terminate evolution. In some runs this condition is never met, and the evolution is terminated when the primary star almost reaches core collapse. In some cases we do follow the system after the companion enters the envelope of the giant star, i.e., the system enters a CEE, although the calculation is much less accurate in that case. When the companion enters the envelope the simple tidal formulae do not hold any more as the envelope is highly distorted (see simulations cited in section 1.2). As well, the accretion processes involves now the Bondi-Hoyle-Lyttleton type flow, and the formulae of the RLOF are not accurate.

In some simulations we do not introduce jets even when the two stars enter a CEE. These serve for comparison. In other cases we do introduce jets according to the assumption of the GEE (section 1.2). In both classes of simulations the mass transfer rate due to RLOF, \dot{M}_{KR} , is according to Kolb & Ritter (1990). In most cases we assume that only a fraction $f_{\text{acc,RL}} = 0.3$ of this mass is accreted, and the rest is lost by the system, a fraction of $f_{\text{L,RL},1} = 0$ is lost from the primary giant star, and a fraction of $f_{\text{L,RL},2} = 0.7$ is lost by the secondary (mass accreting) star. The relation $f_{\text{acc,RL}} + f_{\text{L,RL},1} + f_{\text{L,RL},2} = 1$ holds. In two runs that we present in section 3.3 we take $f_{\text{acc,RL}} = 1$.

Jets that the secondary star launches remove mass, according to our assumption, from the primary envelope and from the acceleration zone of its wind. We assume that jets remove mass when the orbital separation is

$$a < f_{\text{GEE}} (R_1 + R_2), \quad (2)$$

where here $R_2 = 0$, and f_{GEE} is the jet-activity separation factor for which we take values of $f_{\text{GEE}} = 1.1 - 1.5$ in the different runs. When the condition of equation (2) is met, then in addition to the mass transfer \dot{M}_{KR} and mass loss rates of $f_{\text{L,RL},1}\dot{M}_{\text{KR}}$ and $f_{\text{L,RL},2}\dot{M}_{\text{KR}}$ from the primary and secondary stars, respectively, we include extra mass loss resulting from the effect of the assumed jets. The expression for the total jet-driven mass loss rate is

$$\dot{M}_{\text{L,jet}} = f_{\text{jet}}\dot{M}_{\text{KR}} \frac{f_{\text{GEE}} - a/R_1}{f_{\text{GEE}} - 1}; \quad \frac{a}{R_1} < f_{\text{GEE}}, \quad (3)$$

where f_{jet} is the jet-driven mass loss factor, and we calculate cases with $f_{\text{jet}} = 2$ or $f_{\text{jet}} = 4$. Half of the mass loss due to jets is from the giant primary star and half from the secondary star.

We take these values for f_{jet} from the following consideration. The secondary star accretes at a rate of $\dot{M}_{2,\text{acc}} = f_{\text{acc,RL}}\dot{M}_{\text{KR}}$, in our simulations. We assume that the secondary launches a fraction of $\eta_j \approx 0.2$ of the accreted mass in jets, and that the jets have a velocity of about the escape velocity from the secondary star, $v_j \simeq 700 \text{ km s}^{-1}$. The escape velocity from the surface of the giant star in our simulations at the relevant time is $v_1 \simeq 100 \text{ km s}^{-1}$. For a maximum efficiency of energy conversion from jets to envelope removal, the jets can remove a mass at a rate of $\dot{M}_{\text{rem}} \approx \eta_j (v_j/v_1)^2 f_{\text{acc,RL}}\dot{M}_{\text{KR}}$, which we can scale to read

$$\frac{\dot{M}_{\text{rem}}}{\dot{M}_{\text{KR}}} \approx 3 \left(\frac{\eta_j}{0.2} \right) \left(\frac{f_{\text{acc,RL}}}{0.3} \right) \left(\frac{v_j}{7v_1} \right)^2. \quad (4)$$

This corresponds to $f_{\text{jet}} \approx 3$ when the mass removal occurs for $a = R_1$. The highest mass removal by jets that equation (3) gives is when the secondary enters the giant envelope. At that stage the interaction becomes more complicated and the efficiency might increase even more (section 3.3).

We found that we need to reduce the time step when the jet activity begins. We did so by setting the MESA variable `varcontrol_target` to 10^{-5} (instead of the default value, 10^{-4}).

The scheme for mass loss by winds follows de Jager et al. (1988) when the effective surface temperature T_{eff} is below 10^4 K. For hot phases ($T_{\text{eff}} \geq 1.1 \times 10^4$ K) we follow Vink et al. (2001) if the surface hydrogen mass fraction X_s is above 0.4 or Vink (2017) when $X_s \leq 0.4$. For 1.1×10^4 K $> T_{\text{eff}} > 10^4$ K we interpolate.

3 RESULTS

3.1 Preventing the CEE and forming SNe Iib

Our aim in this subsection is to show that under the assumptions of the GEE, in some cases jets might prevent the system from entering a CEE and by that form a progenitor of a SN Iib. For that we present the evolution of the orbital separation and masses of a binary system in two cases. In one case we ignore any effects of jets and find that the system enters a CEE. In the other case we introduce an enhanced mass loss rate by jets according to the assumptions of the GEE, and find that the system does not enter a CEE, and that the primary star reaches core collapse when its hydrogen content is that of a SN Iib.

We first present the evolution of a binary system with an initial circular orbit with a radius of $a_0 = 1000R_{\odot}$, and initial masses of $M_{1,0} = 15M_{\odot}$ and $M_{2,0} = 2.5M_{\odot}$. The primary starts with no rotation. In run `Jet($a_0, f_{\text{GEE}}, f_{\text{jet}}$)=Jet(1000,1.2,4)` we turn on the jets according to equation (3) with $f_{\text{GEE}} = 1.2$ and $f_{\text{jet}} = 4$. In run `NoJet(1000)` we do not consider jets. In section 2 we list the other parameters of the simulations. In all runs presented in sections 3.1 and 3.2 $f_{\text{acc,RL}} = 0.3$, i.e., the secondary star accretes 30% of the mass that the primary star transfers to it in the RLOF process.

We present the evolution of the masses and of the orbital separation with time for the two cases in Fig. 1. To present the entire evolution on one graph, we split the horizontal time axis to three segments, each of a different timescale. Initially the stars have a weak interaction between them and the orbital separation does not change much. At about $t = 1.213675 \times 10^7$ yr, the ratio R_1/a becomes large enough for tidal interaction to act fast. Tidal forces transfer orbital angular momentum to the spin of the giant star, and the orbital separation rapidly decreases. Without jets the system enters a CEE as we mark on the figure, where we terminate the evolution (end of thick-red and thick-green lines). In the case with jets, as depicted by the thin-black lines, the system does not enter a CEE, and the two stars are detached at explosion (end of graph). Although the jets are active for only four years (thick magenta line on the middle horizontal axis) they manage to prevent the CEE (more in section 3.2).

The jets prevent the CEE by removing mass from the

system (section 2), a process that acts to increase the orbital separation. If the ratio of orbital separation to primary (giant) radius, a/R_1 , increases, the effect of the jets decreases (equation 3) and tidal forces decrease back this ratio. If the ratio a/R_1 decreases then the mass removal rate by jets increases, a process that acts to increase orbital separation. The outcome, as the GEE requires (Soker 2015), is that the orbital separation and primary radius are very close to each other during the GEE, as we see in the upper panel of Fig. 1 in the last part of the middle time segment. During part of this time jets are active, and in the rest the RLOF keeps the orbital separation and primary radius such that they evolve close to each other. The final orbital separation is much smaller than the maximum radius the primary star has achieved.

During the GEE the secondary star increases its mass, almost doubling it (thin blue line in the lower panel). To prevent the expansion of the secondary star as a result of the high mass accretion, the jets must carry out large amounts of energy and to remove high entropy gas from the vicinity of the secondary star (Shiber et al. 2016; Chamandy et al. 2018). As Abu-Backer et al. (2018) already noted, the rotation of the accreting star (which we do not treat here) complicates the accretion process (e.g., Kunitomo et al. 2017). This process deserves its own study, but at present we note the following (see also Abu-Backer et al. 2018). Any large envelope that the secondary star might inflate will have high entropy. The jets will remove a large fraction of this envelope, i.e., the jets will remove high entropy gas that will limit the expansion of the envelope of the secondary star. Also, it is possible that the dense accretion disk allows the envelope to inflate along the polar directions, but the accretion process through the dense thin accretion disk continues, and therefore the jets are still active. In any case, for our results to hold, it will be necessary to show by simulating the accretion process, that main sequence stars in the mass range $\approx 1.5 - 3M_{\odot}$ can double their mass and still launch energetic jets.

After the jets activity (the GEE) ends, the system continues to interact via RLOF. This is seen in Fig. 1 by the changing stellar masses that continues after the GEE ends. At the end it is only the wind that removes part of the left-over envelope of the primary star. The main activity of the GEE is to prevent the CEE, and by that allowing the formation of a SN Iib progenitor. At the end of the GEE the hydrogen mass is $M_{\text{GEE,H}} = 4.3M_{\odot}$, at the end of the final RLOF the hydrogen mass is $M_{\text{RLOF,H}} = 0.256M_{\odot}$, while at core collapse it is $M_{\text{CCSN,H}} = 0.058M_{\odot}$, fitting a SN Iib progenitor.

In Fig. 2 we present the evolution of the primary star of the `Jet(1000,1.2,4)` case on the HR diagram, from the main sequence to core collapse. The period during which the jets are active, i.e., the GEE, is mark by a thick-red line. As evident from both Fig. 1 and Fig. 2 the SN Iib we obtain here is a blue-compact progenitor (a radius of about $16R_{\odot}$) as are most progenitors of SNe Iib (e.g., Yoon et al. 2017).

3.2 Numerical limitations

There are several numerical limitations in our usage of the MESA BINARY code in relation to mimicking the GEE. The

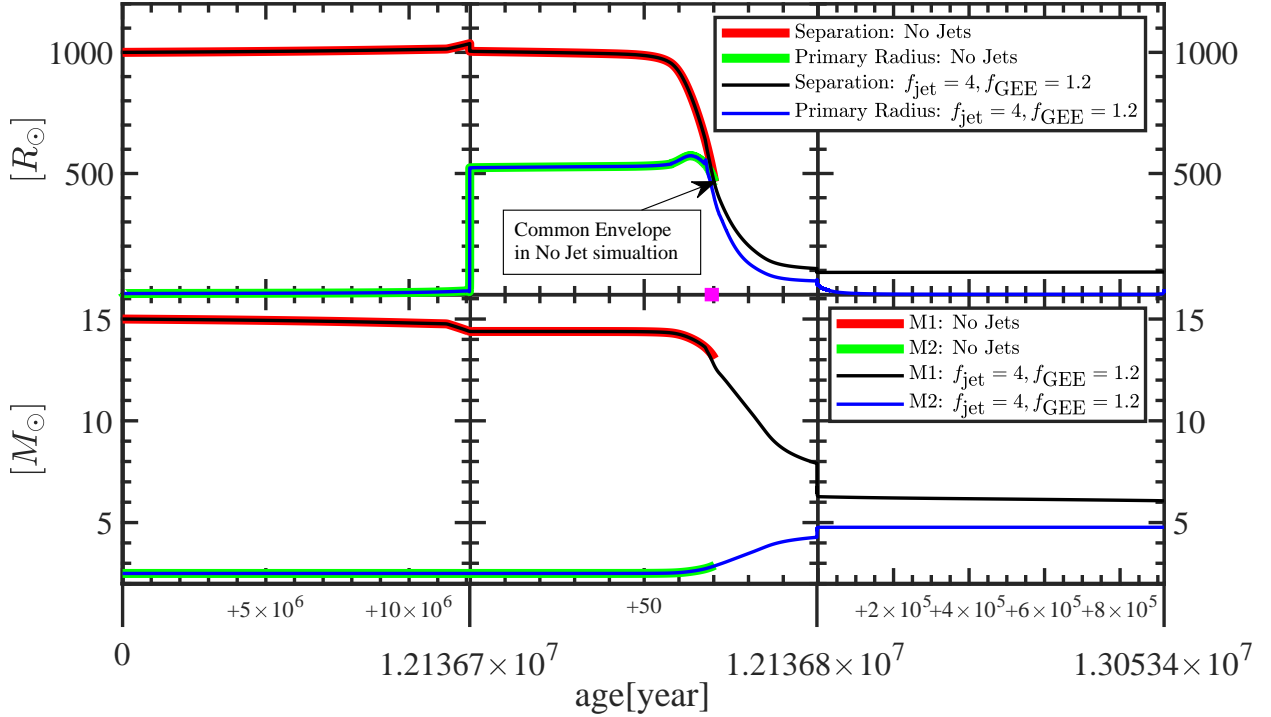


Figure 1. Evolution of orbital separation and primary radius (upper panel) and masses (lower panel) from the zero age main sequence to core collapse of the primary star for the Jet($a_0, f_{\text{GEE}}, f_{\text{jet}}$)=Jet(1000,1.2,4) and NoJet(1000) cases. The horizontal time axis has three segments with different timescales. Each lower large number gives the time in years from the zero age main sequence to the respective large tick that marks the beginning of the time segment, while the smaller numbers closer to the axis give the extra time in years from the beginning of the time segment. The thick red line in the upper panel shows the orbital separation for the NoJet(1000) case where jet activity does not take place. The system enters a common envelope phase and the calculation is terminated. The thin black line presents the orbital separation for the Jet(1000,1.2,4) case, where jet activity takes place when $a < f_{\text{GEE}}R_1$, with $f_{\text{GEE}} = 1.2$, according to equation (3). The short thick magenta horizontal line on the boundary between the two panels marks the jets’ activity period, about four years.

two main problems are the large number of free parameters and the problem in dealing with systems that enter the CEE.

The GEE is a complicated interaction. We here mimic the role of the jets with several free parameters. These are the form of equation (3), the intensity f_{jet} , the initial orbital separation of jet activity $R_1 f_{\text{GEE}}$, and the fraction of mass that is lost from each star (here we use half from each star). In addition, there are also the parameters of the RLOF, e.g., $f_{\text{acc,RL}}$. As we have no good handle of these parameters, it is too early to conduct a systematic study of the parameter space.

The other problem is that the code does not handle well the evolution after the system enters the CEE, and it becomes almost impossible to include our mimicking of the GEE when the secondary star enters the envelope (for that we need full 3D hydrodynamical simulations). We actually expect that in many cases when the secondary star does enter the CEE, the jets, or even the RLOF itself, will be very efficient at removing mass (Shiber et al. 2017; Shiber & Soker 2018; López-Cámara et al. 2019; Shiber et al. 2019) and in some cases the system will exit the CEE and will experience the GEE. This is particularly so when the primary rapidly expands and engulfs the secondary star, because in that case the very outer envelope is of very low density. Although in

the case we present in section 3.1 the jets are active only for 4 years, in reality we expect a longer activity while the secondary star enters the very outskirts of the giant envelope (see simulations cited above).

In many cases when we turn on the jets they remove mass from the giant primary star, something that causes the primary star to expand and swallow the secondary star. In most cases we terminate the simulation at this stage for numerical reasons. But as stated, we actually expect the system to experience the GEE along part of the evolution. Some of these binary systems will end with an orbital separation much smaller than the maximum radius that the primary star has achieved along its evolution, similarly to the case we present in Fig. 1.

Because MESA BINARY cannot properly treat the CEE, namely the evolution of the secondary star inside the giant envelope, we terminate most simulations when the system does enter a CEE. Nonetheless, we do present here in Fig. 3 the evolution of two cases, one with and one without jets, where the system does enter the CEE and then exits the CEE. We take a case, which we term Jet(1000,1.1,4), where we start the jets late when $a < 1.1R_1$, i.e., $f_{\text{GEE}} = 1.1$ in equation (3). All other parameters are as in the Jet(1000,1.2,4) case that we present in section 3.1 and in

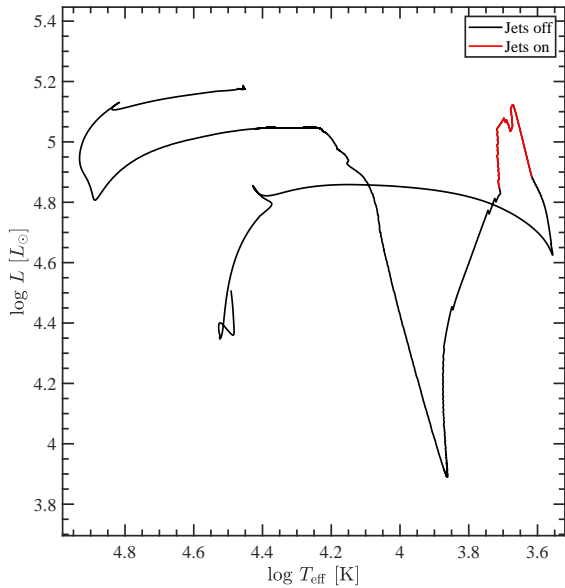


Figure 2. Evolution of the primary star in the Jet(1000,1.2,4) case on the HR diagram. The thick-red line marks the activity period of the jets (see also Fig. 1). We obtain a blue-compact SN I Ib progenitor with a hydrogen mass of $M_{\text{CCSN,H}} = 0.058M_{\odot}$ at core collapse.

Fig. 1. The case without jets is the same as the NoJet(1000) case that we present there. The results of these runs should be taken with very great caution because MESA BINARY cannot properly treat the CEE. However, we do expect that in the GEE the system can get in and out of the CEE, and so the qualitative behaviour might hold, at least for the case with jets (Soker 2017).

The main results of these runs as evident from Fig. 3 are that the system can remove enough mass to cause the primary star to shrink and cause the system to detach, i.e., exit the CEE, and eventually form a SN I Ib progenitor. In the case without jets the secondary gets deeper into the envelope (compare thick-green line of primary radius and thick-red line of orbital separation), while in the case with jets the secondary only grazes the envelope at four time periods owing to four expansions of the primary star (compare thin-blue line of primary radius and thin-black line of orbital separation). This behaviour of several in-and-out phases is expected in some cases of the GEE. In both cases the hydrogen mass at core collapse is $M_{\text{CCSN,H}} = 0.058M_{\odot}$, fitting a SN I Ib progenitor.

This graph, however, presents another numerical limitation of the scheme we use to mimic the GEE with MESA BINARY. The orbital period of the binary system we use here is $P_{\text{orb}} \simeq 0.86(a/500)^{3/2}$ yr, where a is the orbital separation. We can see that the phases of the GEE last each for about $t_{\text{GEE}} \approx 1$ month, much shorter than the orbital period. The code treats the primary star as a spherical star, which cannot be the case when $t_{\text{GEE}} < P_{\text{orb}}$. This is another reason to treat these results with much caution.

We summarise this section as follows. Although the re-

sults are very crude for the reasons we listed above, they do suggest that some systems might enter a CEE but then exit the CEE and by RLOF and wind mass removal form SN I Ib progenitors. Although the system in the present case exits the CEE and forms a SN I Ib progenitor even without assuming the operation of jets, the jets seem to ease this processes. Our results strengthen the case for an evolution route where some binary systems enter a CEE, but exit from it to form blue-compact SN I Ib progenitors.

3.3 Other cases

We did not conduct a systematic search of the parameter space (see section 3.2). However, we did try about 120 cases with and without jets. For the prescription we use with MESA BINARY and with the jets-induced mass removal according to equation (3) we have some interesting findings that we describe below, comparing to the Jet(1000,1.2,4), Jet(1000,1.1,4) and NoJet(1000) cases that we present in sections 3.1 and 3.2.

If we turn on the jets somewhat earlier than at $a = 1.2R_1$ (i.e., $f_{\text{GEE}} > 1.2$) the results do not change much. The jets are active for somewhat a longer time, e.g., about 10-20 years for $f_{\text{GEE}} = 1.4 - 1.5$. The star ends with a hydrogen mass at core collapse that is similar to the Jet(1000,1.2,4) case that we present in section 3.1.

In the Jet(1000,1.1,4) case that we present in section 3.2 the primary expands as a result of mass removal by jets and for a very short time the system enters a CEE (Fig. 3). If the jets are weaker, $f_{\text{jet}} = 2$ instead of $f_{\text{jet}} = 4$ in run Jet(1000,1.1,4) then the primary expands less and the system avoids a CEE, and ends with a blue-compact SN I Ib progenitor.

The same effect of rapid primary expansion in response to mass removal by jets occurs when we simulate a system with initial orbital separation of $a_0 = 1200R_{\odot}$ instead of $a_0 = 1000R_{\odot}$. The primary swallows the secondary and we terminate the simulation. Here we also expect that the jets will remove mass even when the secondary is inside the outskirts of the primary envelope, and this case also leads to a SN I Ib progenitor. For a case with $a_0 = 800R_{\odot}$ the system does not enter a CEE even without jets because the RLOF starts earlier and removes enough primary mass to prevent CEE. The RLOF followed by the wind, without any jets, reduce the hydrogen mass in the primary star and this leads to the formation of a blue-compact SN I Ib progenitor.

We find also that for a secondary mass of $M_2 = 3M_{\odot}$ instead of $M_2 = 2.5M_{\odot}$ in the cases that we present in Figs. 1-3, even without jets the system avoids a CEE and the RLOF and the later wind remove enough mass to form a blue-compact SN I Ib progenitor.

In a case with $M_2 = 2M_{\odot}$ the evolution to a blue-compact SN I Ib progenitor is different. In Fig. 4 we present the strong interaction time period of the Jet(1000,1.1,4,[2,1]) case, where $a_0 = 1000R_{\odot}$, $f_{\text{GEE}} = 1.1$ (late jet interaction), $f_{\text{jet}} = 4$, as in the Jet(1000,1.1,4) case we present in Fig. 3, but here the secondary mass is $M_2 = 2M_{\odot}$ instead of $2.5M_{\odot}$ as in the other figures, and the fraction of the RLOF mass that the secondary star accretes is $f_{\text{acc,RL}} = 1$, instead of $f_{\text{acc,RL}} = 0.3$ as in all other cases. We also present the case without jets.

We note the following behaviour in Fig. 4. The jets re-

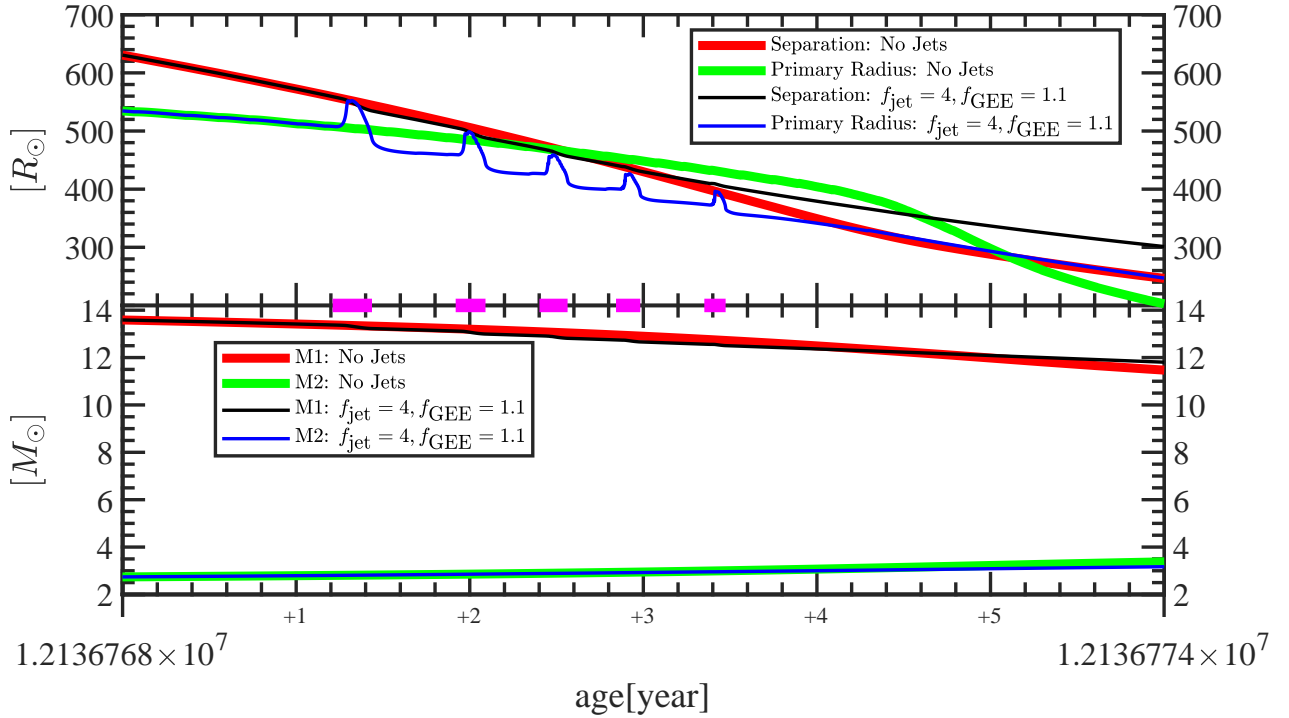


Figure 3. Similar to Fig. 1 but for the Jet(1000,1.1,4) case where the jets are turned on at late time when $a < 1.1R_1$ instead of at $a < 1.2R_1$. We focus on the relevant time period of the evolution when the strong interaction takes place (middle segment of full evolution similar to that in Fig. 1), and continue even after the secondary star enters the envelope, in both cases with and without jets. Note how the primary expands within about a month as a response of mass removal by the jets, and swallows the secondary star. In both cases the system exits the CEE later on, and forms a blue-compact SN I Ib progenitor.

move mass from the primary star and this causes its expansion and the early formation of a CEE (thin lines in the figure), i.e., earlier than the case without jets (thick lines). Both in the case with and without jets the initial spiralling-in takes place on a dynamical time of several months, in what is termed the plunge-in phase of the CEE (e.g., Ivanova et al. 2013b, for a review). Without jets the system continues with the CEE until we terminate the evolution. In the case with jets, on the other hand, the jets remove enough mass and the system exits the CEE and starts a GEE, and then ends with mass removal only by the wind. At core collapse the hydrogen mass is $M_{\text{MCCSN,H}} = 0.062M_{\odot}$. Namely, in the case with jets the system experiences the GEE and leaves a SN I Ib progenitor.

For the reasons we discuss in section 3.2, we should take with caution the results we present in Fig. 4. These reasons include large variations on time-scales shorter or about equal to the dynamical time scale, the inability of the code to treat a non-spherical giant star, and the inaccuracy in the accretion rate when the system enters a CEE. The mass removal rate with jets does however make sense under our assumptions. For $f_{\text{acc,RL}} = 1$ equation (4) gives for the ratio of mass removal rate to mass transfer rate a value of of 10. The maximum ratio we obtain in the Jet(1000,1.1,4,[2,1]) case in our simulation is 16, larger than 10 because $a < R_1$

in equation (3). This makes sense, as when the secondary star enters the envelope the mass accretion rate might be larger than the RLOF.

The results we present above strengthen the finding of sections 3.2 in showing that the GEE can increase the parameter phase for the formation of SN I Ib progenitors.

4 SUMMARY

We used the stellar evolutionary code MESA BINARY to follow the evolution of binary systems that might form SN I Ib progenitors. The new ingredient of the simulations is the introduction of an enhanced mass loss rate due to jets that we assume the secondary star might lunch, according to the assumptions of the GEE (section 1.2). In the present study we mimic the jet-driven mass loss according to equation (3). In section 3.2 we discussed some limitations of the jet-driven mass loss prescription we used, and of the numerical code in general. For example, our results when a binary system experiences a CEE should be treated with high caution, as the numerical code does not handle well such a situation. In all our simulations the initial mass of the primary star is $M_{1,0} = 15M_{\odot}$. We summarise our main findings below.

- (i) As other studies have shown (e.g., Sravan et al. 2018)

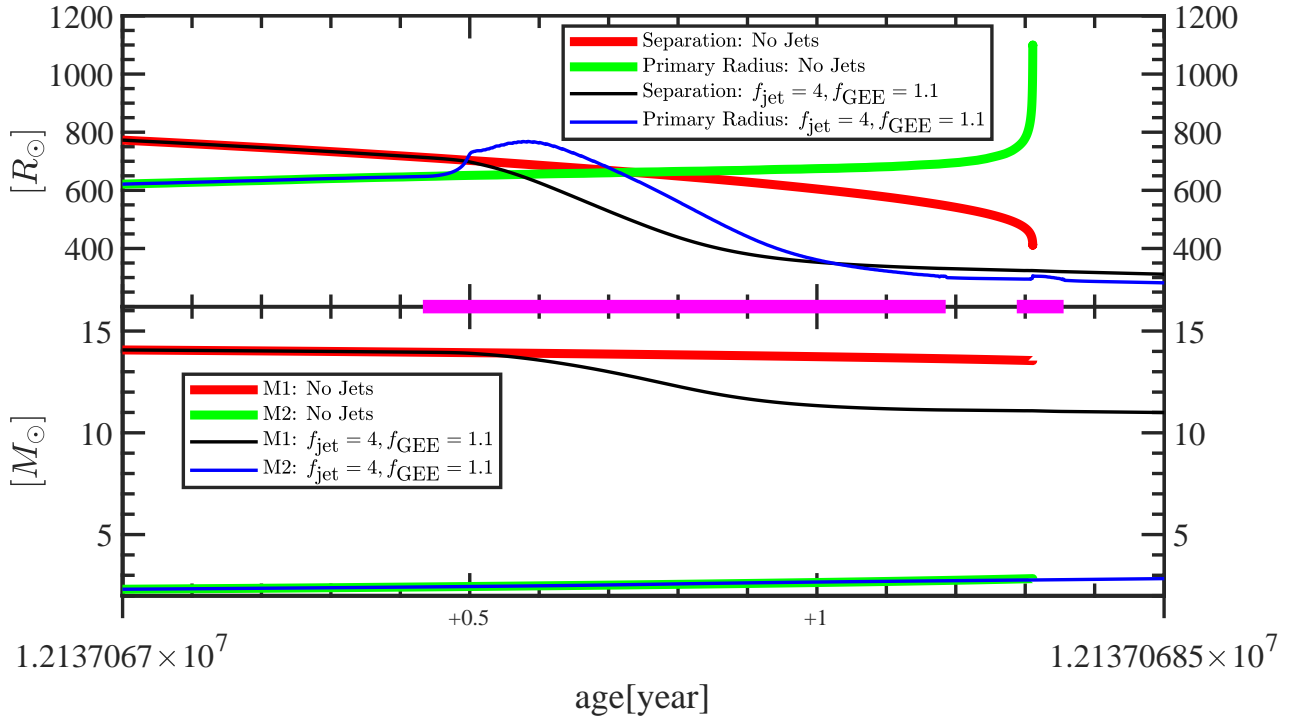


Figure 4. Similar to Fig. 3 but for the Jet(1000,1.1,4,[2,1]) case, that differs from the Jet(1000,1.1,4) case in that the secondary star mass is $M_2 = 2M_\odot$ instead of $M_2 = 2.5M_\odot$, and in that the fraction of the RLOF mass that the secondary star accretes is $f_{\text{acc,RL}} = 1$ instead of $f_{\text{acc,RL}} = 0.3$. In the case with jets the system enters the CEE at an earlier time than the case without jets, but then it exits the CEE to experience a GEE phase, ending with a wind that leaves a hydrogen mass of $M_{\text{MCCSN,H}} = 0.062M_\odot$, which fits a blue-compact SN I Ib progenitor.

in some cases RLOF followed by a wind, even if the secondary star does not launch jets, can remove enough mass to form a SN I Ib progenitor.

(ii) In some cases where without the effect of jets the system does enter a CEE that might prevent the formation of a SN I Ib progenitor, the jet-driven mass loss might prevent the CEE altogether, as in the case that we present in Fig. 1. Because of this jet-driven mass loss, instead of entering a CEE the system experiences a short phase, about four years, of GEE. After that RLOF and then a wind remove most of the envelope mass to leave a blue-compact SN I Ib progenitor (Fig. 2).

(iii) In some cases even without jets the system might enter a CEE and exit from it. RLOF and the wind remove enough mass to form a blue-compact SN I Ib progenitor. Short phase(s) of GEE owing to jet-driven mass loss ease this process as we show in Fig. 3. Sravan et al. (2018) assume that the hydrogen mass at explosion is that when the system enters the CEE. But we found here that in some cases the final hydrogen mass is much lower than that at the onset of the CEE, and can fit that of a SN I Ib progenitor. Namely, this in-and-out of a CEE increases the parameter space of SN I Ib progenitors even before the effects of jets are included.

(iv) In some cases without jet-driven mass loss the binary system enters and does not exit from a CEE. Unless the system experience a fatal CEE that might lead to a SN I Ib progenitor (Lohev et al. 2019; section 1.1), we do not expect

that this system forms a SN I Ib progenitor. The introduction of jet-driven mass loss might bring the system to form a SN I Ib progenitor by exiting it from the CEE into a GEE phase, as we show in Fig. 4.

(v) Overall, our results of the cases we present and tens of other cases that we do not present, show that the process of jet-driven mass loss that leads to episode(s) of GEE phases substantially increases the binary parameter space that leads to the formation of SN I Ib progenitors. This is in accord with the suggestion of Soker (2017) of the GEE scenario for SN I Ib, but some quantitative results are different. For example, we find here the GEE phase to be much shorter than the expectation of Soker (2017). In all the cases we have studied the SN I Ib progenitors are blue-compact ones (rather than yellow or red progenitors).

Our results bring us to try to crudely estimate the fraction of massive CCSN progenitors that experience the GEE. We proceed as follows. Following our discussion in section 1 we assume that post-AGB stars with intermediate orbital periods (post-AGBIB stars) are formed by the GEE. We further assume that the post-red giant branch (post-RGB) stars that Kamath et al. (2016) study and have similar properties to post-AGBIB stars are also formed by the GEE. Kamath et al. (2016) estimate that these post-RGB stars comprise a fraction of 0.0045 of all RGB stars. We also note that the fraction of binary (and higher multiple-stellar systems) of CCSN progenitors is about twice that of solar-like

stars (e.g., Moe, & Di Stefano 2017). These numbers bring us to conclude that $\approx 1\%$ of CCSN progenitors experience the GEE under our assumptions. This amounts to $\approx 10\%$ of SNe I Ib. Sravan et al. (2018) conclude that at solar metallicity their binary channel can account for 0 – 2% of all CC-SNe being SNe I Ib. We estimate that the fraction of SN I Ib progenitors that experience the GEE is about equal to that of binary systems that do not experience the GEE. Namely, the GEE might account for $\approx 0\text{--}2\%$ of the CCSNe becoming SNe I Ib.

Soker (2019) estimates that the fatal CEE scenario (Lohev et al. 2019) might account for 1 – 3% of all CCSNe. Recent studies suggest that single star channels also contribute to the formation of SNe I Ib (e.g., Sravan et al. 2018).

These numbers from the four SN I Ib channels add up to be below the required $\approx 11\%$ fraction of SNe I Ib out of all CCSNe. We therefore re-scale these numbers to reach the required $\approx 11\%$ fraction of SNe I Ib out of all CCSNe. Namely, we argue that the different channels must contribute more than what simple (and conservative) estimates (as we listed above) give. This more optimistic estimate is based also on the conclusion (e.g., Gilkis et al. 2019) that the post-RLOF mass loss rate by wind should be lower than what most studies have assumed, and this increases the number of SN I Ib progenitors by channels that involve RLOF. This brings us to suggest, for solar metallicity at least, that each of the following four SN I Ib progenitor channels contributes about the same, that is, each channel contributes $\approx 2\text{--}4\%$ of all CCSNe, to the formation of SNe I Ib: (1) The binary evolution channel with RLOF but without GEE; (2) the GEE; (3) the fatal-CEE; and (4) the single-star channel.

ACKNOWLEDGMENTS

This research was partially supported by the Israel Science Foundation and by a grant from Prof. Amnon Pazy Research Foundation. AG gratefully acknowledges the generous support of the Blavatnik Family Foundation.

REFERENCES

- Abu-Backer, A., Gilkis, A., & Soker, N. 2018, *ApJ*, 861, 136
- Aldering, G., Humphreys, R. M., & Richmond, M. 1994, *AJ*, 107, 662
- Blackman, E. G., & Lucchini, S. 2014, *MNRAS*, 440, L16
- Chamandy L., Blackman E. G., Frank A., Carroll-Nellenback J., Zou Y., Tu Y., 2019, arXiv, arXiv:1908.06195
- Chamandy, L., Frank, A., Blackman, E. G., et al. 2018, *MNRAS*, 480, 1898
- Chevalier, R. A., & Soderberg, A. M. 2010, *ApJ*, 711, L40
- Claeys, J. S. W., de Mink, S. E., Pols, O. R., Eldridge, J. J., & Baes, M. 2011, *A&A*, 528, A131
- de Jager, C., Nieuwenhuijzen, H., & van der Hucht, K. A. 1988, *A&AS*, 72, 259
- De Marco, O., & Izzard, R. G. 2017, *Publ. Astron. Soc. Australia*, 34, e001
- De Marco, O., Passy, J.-C., Moe, M., Herwig, F., Mac Low, M.-M., & Paxton, B. 2011, *MNRAS*, 411, 2277
- Fox, O. D., Azalee Bostroem, K., Van Dyk, S. D., et al. 2014, *ApJ*, 790, 17
- Fremling, C., Ko, H., Dugas, A., et al. 2019, *The Astrophysical Journal*, 878, L5
- Galaviz, P., De Marco, O., Passy, J.-C., Staff, J. E., & Iaconi, R. 2017, arXiv:1702.07872
- Gilkis, A., Vink, J. S., Eldridge, J. J., & Tout, C. A. 2019, *MNRAS*, 486, 4451
- Gorlova, N., Van Winckel, H., Gielen, C., et al. 2012, *A&A*, 542, A27
- Gorlova, N., Van Winckel, H., Ikonnikova, N. P., Burlak, M. A., Komissarova, G. V., Jorissen, A., Gielen, C., Debusscher, J., & Degroote, P. 2015 *MNRAS*, 451, 2462
- Graur, O., Bianco, F. B., Modjaz, M., Shivvers, I., Filippenko, A. V., Li, W., Smith, N. 2017b, *ApJ*, 837, 121
- Hurley, J. R., Tout, C. A., & Pols, O. R. 2002, *MNRAS*, 329, 897
- Hut, P. 2002, *A&A*, 99, 126
- Iaconi, R., Reichardt, T., Staff, J., De Marco, O., Passy, J.-C., Price, D., Wurster, J., & Herwig, F. 2017, *MNRAS*, 464, 4028
- Ivanova, N., Justham, S., Chen, X., et al. 2013b, *A&ARv*, 21, 59
- Ivanova, N., & Nandez, J. L. A. 2016, *MNRAS*, 462, 362
- Kamath D., Wood P. R., Van Winckel H., Nie J. D., 2016, *A&A*, 586, L5
- Kastner, J. H., Buchanan, C., Sahai, R., Forrest, W. J., & Sargent, B. A. 2010, *AJ*, 139, 1993
- Kilpatrick, C. D., et al. 2017, *MNRAS*, 465, 4650
- Kolb, U., & Ritter, H. 1990, *A&A*, 236, 385
- Kunitomo, M., Guillot, T., Takeuchi, T., & Ida, S. 2017, *A&A*, 599, A49
- Kuruwita, R. L., Staff, J., & De Marco, O. 2016, *MNRAS*, 461, 486
- Lohev, N., Sabach, E., Gilkis, A., & Soker, N. 2019, arXiv:1904.05592
- López-Cámara, D., De Colle, F., & Moreno Méndez, E. 2019, *MNRAS*, 482, 3646
- MacLeod, M., & Ramirez-Ruiz, E. 2015, *ApJ*, 803, 41
- Manick, R., Van Winckel, H., Kamath, D., Hillen, M., & Escorza, A. 2017, *A&A*, 597, A129
- Matheson, T., Filippenko, A. V., Ho, L. C., Barth, A. J., & Leonard, D. C. 2000, *AJ*, 120, 1499
- Meynet, G., Chomienne, V., Ekström, S., et al. 2015, *A&A*, 575, A60
- Meynet, G., & Maeder, A. 1997, *A&A*, 321, 465
- Moe, M., & Di Stefano, R. 2017, *ApJS*, 230, 15
- Nandez, J. L. A., & Ivanova, N. 2016, *MNRAS*, 460, 3992
- Nandez, J. L. A., Ivanova, N., & Lombardi, J. C., Jr. 2014, *ApJ*, 786, 39
- Nie, J. D., Wood, P. R., & Nicholls, C. P. 2012, *MNRAS*, 423, 2764
- Ohlmann, S. T., Röpke, F. K., Pakmor, R., & Springel, V. 2016, *ApJ*, 816, L9
- Oomen, G.-M., Van Winckel, H., Pols, O., Nelemans, G., Escorza, A., Manick, R., Kamath, D., & Waelkens, C. 2018, arXiv:1810.01842
- Ouchi, R., & Maeda, K. 2017, arXiv:1705.02430
- Passy, J.-C., De Marco, O., Fryer, C. L., et al. 2012, *ApJ*, 744, 52
- Paxton, B., Bildsten, L., Dotter, A., Herwig, F., Lesaffre, P., & Timmes, F. 2011, *ApJS*, 192, 3
- Paxton, B., Cantiello, M., Arras, P., et al. 2013, *ApJS*, 208, 4
- Paxton, B., Marchant, P., Schwab, J., et al. 2015, *ApJS*, 220, 15
- Paxton, B., Schwab, J., Bauer, E. B., et al. 2018, *ApJS*, 234, 34
- Podsiadlowski, P., Hsu, J. J. L., Joss, P. C., & Ross, R. R. 1993, *Nature*, 364, 509
- Reichardt, T. A., De Marco, O., Iaconi, R., et al. 2019, *MNRAS*, 484, 631
- Ricker, P. M., & Taam, R. E. 2012, *ApJ*, 746, 74
- Sabach, E., & Soker, N. 2015, *MNRAS*, 450, 1716
- Shiber, S., Iaconi, R., De Marco, O., & Soker, N. 2019, *MNRAS*, 1953
- Shiber, S., Kashi, A., & Soker, N. 2017, *MNRAS*, 465, L54
- Shiber, S., Schreier, R., & Soker, N. 2016, *Res. Astron. Astrophys.*, 16, 117

- Shiber S., Soker N., 2018, MNRAS, 477, 2584
- Shivvers, I., Modjaz, M., Zheng, W., et al. 2017, arXiv:1609.02922
- Smith, N., Li, W., Filippenko, A. V., & Chornock, R. 2011, MNRAS, 412, 1522
- Soker, N. 2015, ApJ, 800, 114
- Soker, N. 2016, New Astron. Rev., 75, 1
- Soker, N. 2017, MNRAS, 470, L102
- Soker, N. 2019, Sci. China Phys. Mech. Astron., 62, 9501
- Stravan, N. 2016, 41st COSPAR Scientific Assembly, 41,
- Stravan, N., Marchant, P., & Kalogera, V. 2018, arXiv:1808.07580
- Staff, J. E., De Marco, O., Macdonald, D., Galaviz, P., Passy, J.C., Iaconi, R., & Mac Low, M.-M 2016a, MNRAS, 455, 3511
- Staff, J. E., De Marco, O., Wood, P., Galaviz, P., & Passy, J.-C. 2016b, MNRAS, 458, 832
- Stancilffe, R. J., & Eldridge, J. J. 2009, MNRAS, 396, 1699
- Taam, R. E., & Ricker, P. M. 2010, New Astron. Rev., 54, 65
- Thomas, J. D., Witt, A. N., Aufdenberg, J. P., Bjorkman, J. E., Dahlstrom, J. A., Hobbs, L. M., & York, D. G. 2013, MNRAS, 430, 1230
- Van Winckel, H. 2017a, Edited by Anatoly Miroshnichenko, Sergey Zharikov, Daniela Korkov and Marek Wolf. ASP Conference Series, Vol. 508. San Francisco: Astronomical Society of the Pacific, 2017, p.197
- Van Winckel, H. 2017b, in Planetary Nebulae: Multi-Wavelength Probes of Stellar and Galactic Evolution, Proceedings IAU Symposium No. 323, p. 231, eds. X. Liu, L. Stanghellini, and A. Karakas A.C.
- Vink, J. S. 2017, A&A, 670, L8
- Vink, J. S., de Koter, A., & Lamers, H. J. G. L. M. 2001, A&A, 369, 574
- Witt, A. N., Vijn, U. P., Hobbs, L. M., Aufdenberg, J. P., Thornburn, J. A., & York, D. G. 2009, ApJ, 693, 1946
- Woosley, S. E., Eastman, R. G., Weaver, T. A., & Pinto, P. A. 1994, ApJ, 429, 300
- Yoon, S.-C., Dessart, L., & Clocchiatti, A. 2017, ApJ, 840, 10